International Journal of Current Advanced Research
ISSN: O: 2319-6475, ISSN: P: 2319-6505, Impact Factor: 6.614
Available Online at www.journalijcar.org
Volume 8; Issue 03 (F); March 2019; Page No.17921-17934
DOI: http://dx.doi.org/10.24327/ijcar.2019.17934.3416

Research Article

EVALUATINGPROPERTIES OF FREE BASE, CATIONIC AND HYDROCHLORIDE SPECIES OF POTENT PSYCHOTROPIC 4-BROMO-2,5-DIMETHOXYPHENETHYLAMINE DRUG

María Eugenia Manzur, Roxana A. Rudyk and Silvia Antonia Brandán*

Cátedra de Química General, Instituto de Química Inorgánica, Facultad de Bioquímica. Química y Farmacia, Universidad Nacional de Tucumán, Ayacucho 471, (4000) San Miguel de Tucumán, Tucumán, Argentina

A R T I C L E I N F O

Article History:
Received 6th December,, 2018
Received in revised form 15th January, 2019
Accepted 12th February, 2019
Published online 28th March, 2019

Key words:
4-Bromo-2,5 dimethoxyphenethylamine,structural properties, force fields, vibrational analysis, DFT calculations.

A B S T R A C T

The structural, electronic, topological and vibrational properties of free base, cationic and hydrochloride species of potent psychotropic 4-Bromo-2,5-dimethoxyphenethylamine (2C-B) drug have been evaluated combining the experimental available IR, ATR, Raman, 1H-, 13C-NMR and ultraviolet-visible spectroscopies with DFT calculations by using the hybrid B3LYP/6-31G* method. The properties were predicted in gas phase and in aqueous solutions by using the polarized continuum (PCM) and the universal solvation model. The cationic species of 2C-B shows higher solvation energy, presenting values approximately similar to morphine, scopolamine and heroin alkaloids. NBO calculations suggest that hydrochloride species is most stable in solution while the AIM studies reveal that in the hydrochloride species in gas phase the H-Cl bond shows covalency while in solution is ionic. The gap value for the hydrochloride species in solution is similar to observed for cocaine. The cationic species of 2C-B has a global electrophilicity index higher than some alkaloids. The expected 78, 81 and 84 normal vibration modes for free base, cationic and hydrochloride species of 2C-B were assigned with the corresponding harmonic force fields by using SQMFF methodology. The force constants are reported. The bands observed in the predicted UV-Vis spectra for the free base and hydrochloride species evidence that the cationic species is clearly present in solution, as compared with the experimental ones.

INTRODUCTION

The compound 4-Bromo-2,5-dimethoxyphenethylamine, commonly known as 2C-B, is a psychedelic phenylethylamine derivative which is a psychotropic drug with effects on humans not yet fully known although some biological studies suggest that it is an abuse drug, as tropane alkaloids [1-12]. Some recent studies on 2C-B indicate toxicological and neuropsychiatric symptoms, including typical hallucinations [1,2,4]. Multiple studies of that phenylethylamine derivative related to the effects and biological activities on animal and humans were published but, so far, their experimental structure and chemical, electronic, topological and vibrational properties are not available. Structurally for 2C-B, three species can be expected, as in the tropane alkaloids [13-19], which are free base, cationic and hydrochloride species although the main difference with the tropane alkaloids is that the free base is a primary amine whiles the cationic species is an ammonium cation. In the alkaloids those three species contain the N-CH_3 group forming tertiary amines.

Corresponding author:* **Silvia Antonia Brandán
Cátedra de Química General, Instituto de Química Inorgánica, Facultad de Bioquímica. Química y Farmacia, Universidad Nacional de Tucumán, Ayacucho 471, (4000) San Miguel de Tucumán, Tucumán, Argentina

In the species of 2C-B there are two O-CH_3 groups and a Br atom in the phenyl ring different from the alkaloids. On the other hand, techniques as High performance liquid chromatography (HPLC) equipped with mass Mass Spectrometry, Nuclear Magnetic Resonance Spectroscopy, ultraviolet visible, infrared and Raman spectra are employed to analyse and identify 2C-B [8,11,12]. So far, the identifications of all bands observed in the vibrational spectra were not performed. Hence, the great interest to study it interesting methamphetamine species. The structural studies of free base, cationic and hydrochloride species of 2C-B are very important to find the most stable structures in order to perform their vibrational assignments. Besides, the structural, electronic and topological properties of those three species of 2C-B are also important to explain their biological properties and mechanism of action of this drug because there are other species, as diphenhydramine, cyclizine, and promethazine, despite have N-CH_3 groups they present antihistaminic properties [20-22].Due to this set of backgrounds our objectives in this work are: (i) to optimize the three structures of 2C-B in gas phase and in aqueous solution by using density functional theory (DFT) with the hybrid B3LYP/6-31G* method, (ii) to study the atomic charges, molecular electrostatic potentials, bond orders, stabilization energies and topological properties at the same level of theory, (iii) to compare the experimental available infrared and Raman spectra of 2C-B with the

corresponding predicted and, then to perform the complete vibrational assignments by using the scaled quantum mechanical force field (SQMFF) methodology and the Molvib program, (iv) to predict the reactivities and behaviours of three species of 2C-B by using the frontier orbitals and finally, (v) to compare the obtained properties with those reported for tropane alkaloids in order to find correlations or similarities among their properties. Additionally, the ^{1}H- and ^{13}C-NMR and Ultraviolet-visible spectra were also predicted and compared with the corresponding experimental ones.

METHODOLOGY OF CALCULATIONS

The structuresof free base, cationic and hydrochloride species of 2C-B were modelled with the *Gauss View* program [23]and, later, these species were optimized in gas phase and in aqueous solution with the Revision A.02 of Gaussian program [24] by using the hybrid B3LYP/6-31G* method [25,26].All properties were computed with that method because they were compared with those reported for alkaloids with the same method. All species in solution were optimized with the integral equation formalism variant polarised continuum method (IEFPCM) while the solvation energies were computed with the universal solvation model [27-29].The solvation energies for the three species were corrected by zero point vibrational energy (ZPVE). The volumes and their variations were calculated with the Moldraw program [30]. We can see the three structures studied of 2C-B in **Figure 1** together with the atoms labelling.

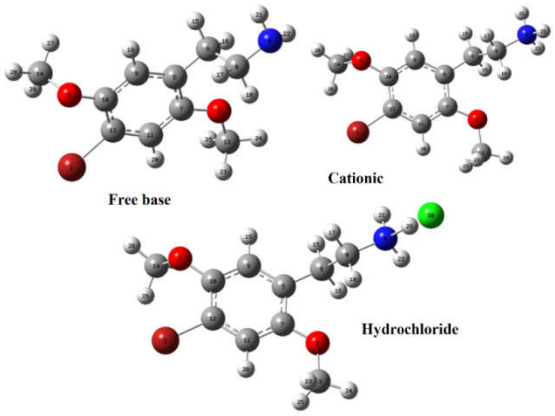

Figure 1 Theoretical molecular structures of free base, cationic and hydrocloride species of 4-Bromo-2,5-dimethoxyphenethylamine and atoms labeling.

The NBO and AIM2000 programs [31-33] together with Merz-Kollman (MK) charges [34] were employed to calculate the atomic natural population (NPA), Mulliken and, molecular electrostatic potentials, bond orders and topological properties. On the other hand, the prediction of reactivities and behaviours of those three species in both media were performed with the frontier orbitals and global descriptors by using the gap values [35-41]. The normal internal coordinates for those three species and transferable scaling factors were used to obtain the harmonic force fields and force constants in both media at the B3LYP/6-31G* level with the scaled quantum mechanical force field (SQMFF) methodology and the Molvib program [42-44]. The Raman spectra predicted in activities were changed to intensities using known equations [45,46]. Potential energy distribution (PED) contributions ≥ 10% were used to perform the vibrational assignments of experimental available infrared and Raman spectra of 2C-B [11,12,47].The ^{1}H and ^{13}C chemical shifts of all species of 2C-B were predicted by using the Gauge-Independent Atomic Orbital (GIAO) method [48] considering to Trimethylsilane (TMS)as reference. Additionally, the ultraviolet-visible spectra of three species were also predicted with Time-dependent DFT calculations (TD-DFT) at the same level of theory and the Gaussian 09 program [24]. Then, these two NMR and UV-Visible spectra were compared with the corresponding experimental ones [11,47].

RESULTS AND DISCUSSION

Properties of Three Speciesin Both Media

Calculated total uncorrected and corrected by zero point vibrational energy (ZPVE) energies, dipole moments and volumes (V) of three species of 2C-B in gas phase and in aqueous solution by using the B3LYP/6-31G* method are shown in **Table 1**. Note that the cationic species present the higher dipole moment values in both media but the hydrochloride species the higher volume values due to the presence of Cl atom in its structure.

Table 1. Calculated total energies (*E*), dipole moments (μ) and volumes (V) of three species of 2C-B in gas and aqueous solution phases.

B3LYP/6-31G* Method				
Medium	**E (Hartrees)**	**ZPVE**	**μ (D)**	**V (Å^3)**
Free base				
GAS	-3166.3655	-3166.1348	3.00	225.8
PCM	-3166.3772	-3166.1467	3.98	225.4
Cationic				
GAS	-3166.7389	-3166.4934	20.72	229.7
PCM[#]	*-3166.8484*	-3166.6030	*25.45*	*228.4*
Hydrochloride				
GAS	-3627.1828	-3626.9427	7.08	253.8
PCM	-3627.2250	-3626.9793	14.85	259.4

[#]Imaginary frequencies

The cationic species in solution has evidenced an imaginary frequency in aqueous solution. Here, the total energy values corrected by ZPVE decrease in both media, as also was observed in the three species of promethazine [22].The hydrochloride species in solution shows an increase in the volume while the free base in this medium exhibit a slight contraction in the volume. In the hydrochloride species, the hydration with water molecules could justify the increase in the dipole moment and volume in solution.

Corrected and uncorrected solvation energies by the total non-electrostatic terms and by zero point vibrational energy (ZPVE) of three species of 2C-B by using the B3LYP/6-31G* method are presented in Table 2where the values are compared with the values for other species. The behaviours of all species can be seen quickly in Figure 2.

Table 2 Corrected and uncorrected solvation energies by the total non-electrostatic terms and by zero point vibrational energy (ZPVE) of three species of 2C-B by using the B3LYP/6-31G* method compared with the same species of other alkaloids.

B3LYP/6-31G* method[a]			
Solvation energy (kJ/mol)			
Condition	ΔG_{un} [#]	ΔG_{ne}	ΔG_{c}
Free base			
2C-B[#a]	-31.21	18.10	-49.31
S(-)-Promethazine[b]	-20.19	15.88	-36.07
R(+)-Promethazine[b]	-3.41	14.46	-17.87

Cyclizine[c]	-23.60	5.93	-29.53
Morphine[d]	-47.74	13.17	-60.91
Cocaine[e]	-42.75	28.51	-71.26
Scopolamine[f]	-56.66	18.81	-75.47
Heroin[g]	-59.54	29.13	-88.67
Tropane[b,h]	-11.80	0.75	-12.55
Cationic			
2C-B[#a]	-287.48	21.21	-308.69
S(-)-Promethazine[b]	-7.08	7.40	-14.48
R(+)-Promethazine[b]	-255.22	7.59	-262.81
Cyclizine[c]	-238.43	5.93	-244.36
Morphine[d]	-282.23	26.96	-309.19
Cocaine[e]	-216.66	38.58	-255.24
Scopolamine[f]	-279.87	30.47	-310.34
Heroin[g]	-280.13	43.01	-323.14
Tropane[b,h]	-228.99	15.34	-244.33
Hydrochloride			
2C-B[#a]	-96.00	26.58	-122.58
S(-)-Promethazine[b]	-101.25	30.81	-70.44
R(+)-Promethazine[b]	-21.51	30.51	-52.02
Cyclizine[c]	-81.57	23.49	105.06
Morphine[d]	-118.82	25.92	-144.74
Cocaine[e]	-99.94	38.20	-138.14
Scopolamine[f]	-95.19	27.55	-122.74
Heroin[g]	-118.56	43.38	-161.94
Tropane[b,h]	-72.13	15.05	-87.18

[#]Imaginary frequencies
[a]This work, [b]From Ref [22], [c]From Ref [21], [d]From Ref [13], [e]From Ref [15], [f]From Ref [19],
[g]From Ref [17],[h]From Ref [14]

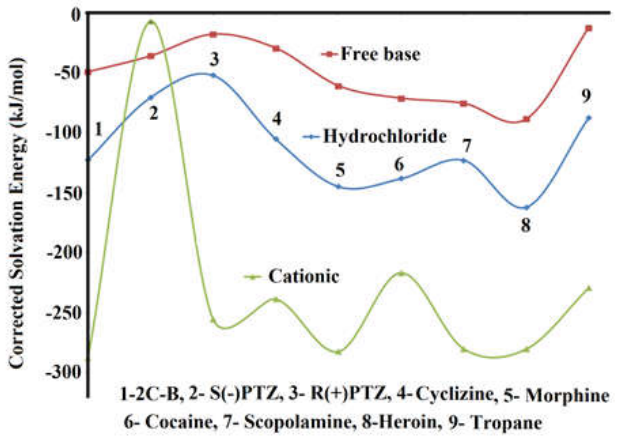

Figure 2 Corrected solvation energies of free base, cationic and hydrocloride species of 2C-B compared with the corresponding to other species by using the B3LYP/6-31G* method.

Analysing deeply Fig. 2 we observed that the cationic species have higher corrected solvation energies, with exception of cationic species of S (-)-Promethazine enantiomer which presents the less negative value. Above studies have evidenced that the hydrochloride species in solution and in solid phase are found as cationic ones and, for these reasons, probably the cationic species present higher solubility for which these species are highly employed in pharmacology. Therefore, the drug absorption is important in the research of pharmaceutical preparations, as reported by Bohloko studying the formulation of an intranasal dosage form for cyclizine hydrochloride [48]. Here, a very interesting result is the higher solvation energy that present the cationic species of 2C-B because its values is approximately similar to those observed for morphine, scopolamine and heroin alkaloids. Moreover, the hydrochloride species of 2C-B shows solvation energy similar to scopolamine alkaloid, as can be seen in Table 2. This property, solvation energy similar to the alkaloids, could possibly justify in part that 2C-B can be an abuse drug and, also, obviously the potent psychotropic activity that was observed in it.

Geometries of three species in both media

Table 3 shows calculated geometrical parameters for those three species of 2C-B in the two media compared with the experimental values determined for (*E*)-*N*-(3,4-dimethoxyphenethyl)-3-methoxybut-2-enamide by X-ray diffraction [49] by using the root-mean-square deviation (RMSD) values.

Table 3 Comparison of calculated geometrical parameters for three species of 2C-B in both media with those experimental determined for (*E*)-*N*-(3,4-dimethoxyphenethyl)-3-methoxybut-2-enamide.

Parameter	B3LYP/6-31G* Method [a]						Experimental[b]
	Free base		Cation		Hydrochloride		
	Gas	PCM	Gas	PCM	Gas	PCM	
Bond lengths (Å)							
Br1-C12	1.909	1.913	1.897	1.912	1.907	1.911	
O2-C7	1.368	1.370	1.371	1.367	1.367	1.368	1.370(2)
O2-C13	1.419	1.430	1.430	1.431	1.421	1.431	1.429(3)
O3-C10	1.374	1.383	1.364	1.382	1.372	1.382	1.366(2)
O3-C14	1.429	1.437	1.438	1.438	1.430	1.438	1.425(3)
N4-C8	1.463	1.468	1.535	1.505	1.476	1.497	1.453(2)
C5-C6	1.510	1.510	1.513	1.512	1.511	1.512	1.505(3)
C6-C8	1.549	1.543	1.528	1.529	1.541	1.531	1.521(3)
RMSD[b]	**0.012**	**0.013**	**0.032**	**0.022**	**0.013**	**0.019**	
Bond angles (°)							
Br1-C12-C10	119.8	119.8	119.8	119.7	119.8	119.7	
Br1-C12-C11	118.9	118.8	118.8	118.8	118.9	118.8	
C7-O2-C13	118.5	118.4	118.2	118.4	118.5	118.4	117.00(18)
C10-O3-C14	114.7	113.9	115.8	113.9	114.8	114.2	116.74(16)
N4-C8-C6	115.5	114.8	110.6	110.2	114.2	111.1	111.08(17)
C8-C6-C5	113.4	113.3	109.9	111.6	112.7	111.7	112.77(17)
RMSD[b]	**2.6**	**2.5**	**1.6**	**1.7**	**2.0**	**1.5**	
Dihedral angles (°)							
N4-C8-C6-C5	179.6	179.2	175.4	177.9	178.4	178.3	177.36(18)
C13-O2-C7-C5	-179.5	178.6	-174.6	0.3	179.6	-177.3	175.8(2)
C13-O2-C7-C11	0.4	-1.4	-174.6	-179.6	-0.3	2.7	-4.2(3)
C14-O3-C10-C12	-84.9	-88.9	-82.1	-88.9	-84.9	-88.7	1.6(3)
C14-O3-C10-C9	97.7	93.3	101.5	93.3	97.8	93.7	-178.34(18)
RMSD[b]	**204.9**	**128.1**	**217.8**	**169.4**	**129.4**	**203.4**	

aThis work, bRef [49]

The experimental molecular structure of (*E*)-*N*-(3,4-dimethoxyphenethyl)-3-methoxybut-2-enamide can be seen in **Figure 3** where are indicated with red circles the common part similar to the three species of 2C-B.Here, the theoretical calculations by using the hybrid B3LYP/6-31G* method show very good concordances with variations for bond lengths between 0.032 and 0.012 Å and for bond angles between 2.6 and 1.5 º.

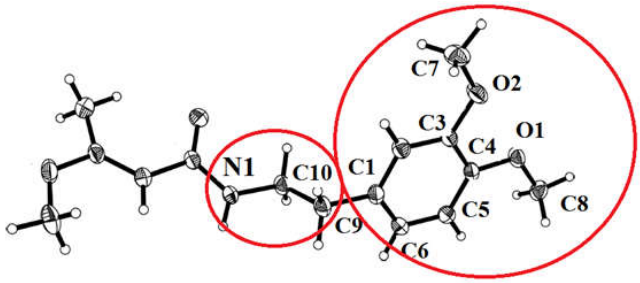

Figure 3. Experimental molecular structure of (*E*)-*N*-(3,4 dimethoxyphenethyl)-3-methoxybut-2-enamide. The moietiesindicated in red circlesare compared with the species of 2C-B.

On the other hand, the higher RMSD differences are observed for dihedral angles (217.8-128.1 º), as can be seen in Table 3. These differences can be clearly explained because the two O-

CH_3 groups linked to phenyl ring in the compared compound are next to each other, different from the species of 2C-B where these groups show an important separation between them, as shown in Figure 1. These results show that the three structures of 2C-B can be clearly used to perform the vibrational assignments.

Charges, Electrostatic Potentials and bond Ordersstudies

Here, the atomic Mulliken, Merz-Kollman(MK) and natural population (NPA) charges, molecular electrostatic potentials (MEP) and bond orders studies (BOs) are very important properties necessary to explain why the cationic species of 2C-B, despite have structures different from morphine, scopolamine and heroin alkaloids, show similar solvation energy values. Therefore, for the three species of 2C-B are expected modifications in the charges and in their distributions. In Table 4 are summarized the three charges studies, the MEP values and the BOs for the three species of 2C-B in both media by using the hybrid B3LYP/6-31G* method. In Table 4 only are presented the values corresponding to the N atoms and to the C and O atoms belonging to both O-CH_3 groups because in these atoms are observed the higher variations. In Figure 4 are graphed the behaviours of three charges on atoms of free base species in the two media while in Figures 5 and 6 are observed the variations in the charges on atoms of hydrochloride and cationic species with the media.

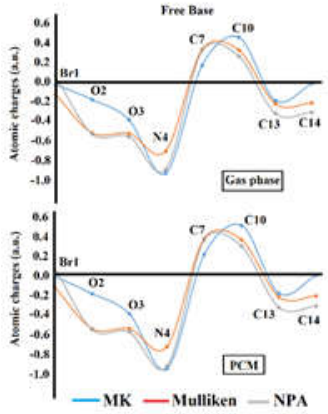

Figure 4 Calculated MK, Mulliken and NPA charges of free base species of 2C-B in both media by using the B3LYP/6-31G* method.

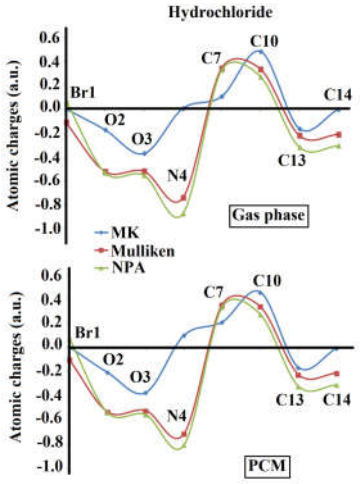

Figure 5 Calculated MK, Mulliken and NPA charges of hydrochloride species of 2C-B in both media by using the B3LYP/6-31G* method.

Table 4 Mulliken, Merz-Kollman and NPA charges, molecular electrostatic potentials (MEP) and bond orders, expressed as Wiberg indexes for three forms of 2C-B in gas phase and in aqueous solution by using B3LYP/6-31G* calculations.

Free base										
	GAS					PCM				
Atoms	MK	Mulliken	NPA	MEP	BO	MK	Mulliken	NPA	MEP	BO
Br1	-0,020	-0,123	0,061	-175,268	1,194	-0,023	-0,122	0,060	-175,269	1,191
O2	-0,175	-0,516	-0,527	-22,273	2,119	-0,187	-0,521	-0,529	-22,273	2,115
O3	-0,380	-0,520	-0,553	-22,297	2,036	-0,382	-0,523	-0,554	-22,298	2,029
N4	-0,927	-0,701	-0,886	-18,372	2,788	-0,906	-0,694	-0,881	-18,372	2,787
C7	0,178	0,339	0,327	-14,672	3,907	0,184	0,340	0,328	-14,671	3,907
C10	0,462	0,331	0,270	-14,681	3,924	0,465	0,329	0,268	-14,680	3,925
C13	-0,185	-0,218	-0,316	-14,674	3,728	-0,184	-0,218	-0,317	-14,673	3,727
C14	-0,010	-0,209	-0,305	-14,691	3,734	-0,012	-0,208	-0,306	-14,690	3,735
Cation										
	GAS					PCM				
Atoms	MK	Mulliken	NPA	MEP	BO					
Br1	0,061	-0,061	0,116	-175,179	1,233					
O2	-0,206	-0,549	-0,552	-22,160	2,094					
O3	-0,381	-0,516	-0,549	-22,206	2,049					
N4	-0,448	-0,734	-0,790	-18,024	3,195					
C7	0,156	0,354	0,325	-14,560	3,906					
C10	0,491	0,346	0,289	-14,578	3,931					
C13	-0,191	-0,234	-0,320	-14,574	3,704					
C14	0,017	-0,223	-0,309	-14,610	3,715					
Hydrochloride										
	GAS					PCM				
Atoms	MK	Mulliken	NPA	MEP	BO	MK	Mulliken	NPA	MEP	BO
Br1	0,001	-0,113	0,070	-175,259	1,200	0,004	-0,100	0,078	-175,250	1,203
O2	-0,172	-0,521	-0,531	-22,261	2,116	-0,205	-0,530	-0,535	-22,247	2,112
O3	-0,372	-0,518	-0,552	-22,288	2,038	-0,371	-0,520	-0,552	-22,279	2,033
N4	0,005	-0,741	-0,874	-18,305	2,951	0,098	-0,712	-0,803	-18,214	3,146
C7	0,105	0,344	0,328	-14,659	3,907	0,207	0,350	0,333	-14,644	3,908
C10	0,482	0,334	0,272	-14,670	3,925	0,453	0,334	0,273	-14,657	3,928
C13	-0,163	-0,221	-0,317	-14,665	3,723	-0,165	-0,225	-0,319	-14,654	3,716
C14	-0,001	-0,211	-0,306	-14,683	3,732	-0,006	-0,212	-0,307	-14,674	3,730

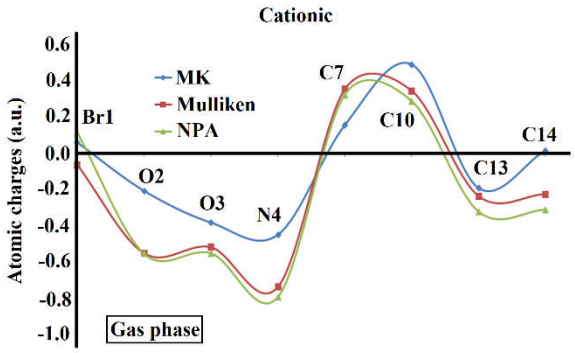

Figure 5 Calculated MK, Mulliken and NPA charges of cationic species of 2C-B in gas phase by using the B3LYP/6-31G* method.

In general, the three figures show that the MK charges on the atoms considered in the three species (blue lines) have behaviours different from the Mulliken and NPA charges and, these two latter charges present practically the same variations. In all cases, the charges on N4 atoms have the most negative values while the charges on C7 and C10 atoms present the most positive ones. The differences observed in the MK charges on the O2 and O3 atoms belonging to the two O-CH_3 groups show different values in the two media indicating clearly that both groups in the three species have different environment, for which, the group next to the side chain (O2-CH_3) evidence less negative charges than those observed on O3 atoms. However, both Mulliken and NPA charges on the two O atoms evidence most negative values on O3 atoms in the three species and in the two media. Hence, the higher values predicted in the C7-O2-C13 bond angles (118.5º) than the C10-O3-C14 bond angles (115.8-113.9º) could be attributed to the MK charges because the repulsion due to the negative MK charges on the O2 and C13 atoms could generate high C7-O2-C13 bond angle, as compared with the C10-O3-C14 bond angles. Thus, the lower values observed in the C10-O3-C14 bond angles could be justified by the difference between the MK charges on the O3 and C14 atoms, too.

If now are analysed the molecular electrostatic potentials (MEP) for the three species of 2C-B in both media from Table 4 there are not significant variations among the species only the expected tendency it is observed: Br > O > N > C > H. But, when the MEP surfaces are mapped and deeply analysed we can see the different red, blue and green colorations typical of nucleophilic, electrophilic and inert regions, respectively. Thus, in Figure 6 are graphed the MEP surfaces of free base, cationic and hydrocloride species of 2C-B in gas phase by using the B3LYP/6-31G* method.

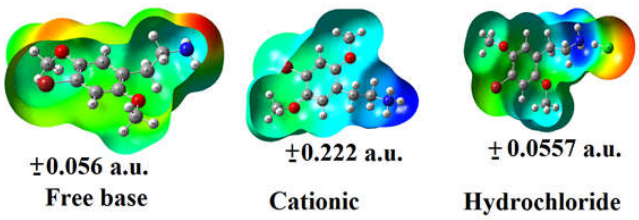

Figure 6 Calculated molecular electrostatic potentials surfaces of free base, cationic and hydrocloride species of 2C-B in both media by using the B3LYP/6-31G* method.

The free base shows strong red colours on the O and N atoms and a sligth orange colour on the Br atom while the ligth blue colours are observed on the H atoms of NH_2 group. The cationic species, on the contrary show strong blue colours on the NH_3^+ group and ligth blue colours on the remains atoms with exception of regions on O and Br atoms where the colorations are sligthly orange. The hydrochloride species shows strong red colour on the Cl atom and light red colours on the Br and O atoms. In this species the strong blue colour is newly located on the NH_3^+ group. These different colorations clearly reveal the sites reacting with potential biological nucleophiles or electrophiles reactive.

From the analysis of bond orders, expressed as Wiberg indexes, from Table 4 it is possible to observe a slight decreasing of values for the free base in solution and both O atoms of hydrochloride species but, in particular, for the hydrochloride species in solution there are increase in the BO of N, C7, C10, C13 and C14 atoms. These changes can be easily attributed to the hydration of NH_3^+ and O-CH_3 groups in these regions with water molecules, as revealed by MEP surfaces.

Natural Bond Orbital (NBO) study

In Table 5 are given the main donor-acceptor energy interactions for the free base and hydrochloride species of 2C-B in both media by using the B3LYP/6-31G* level of theory while in Table 6 are observed the values for the cationic species in gas phase. For the free base in the two media are observed the same three interactions, which are, the $\pi \rightarrow \pi^*$, $n \rightarrow \pi^*$ and $\pi^* \rightarrow \pi^*$ transitions while in the hydrochloride species are observed in gas phase transitions different from in solution. Hence, for this species the four $\pi \rightarrow \pi^*$, $n \rightarrow \sigma^*$, $n \rightarrow \pi^*$ and $\pi^* \rightarrow \pi^*$ transitions are predicted in gas phase while in solution are predicted additionally other two transitions: $\sigma \rightarrow n^*$ and $n \rightarrow n^*$.

Table 5 Main delocalization energies (in kJ/mol) for the free base and hydrochloride species of 2C-Bin gas and aqueous solution phases and by using B3LYP/6-31G* calculations.

B3LYP/6-31G*[a]				
Delocalization	Free base		Hydrochloride	
	Gas	PCM	Gas	PCM
πC5-C9 →π^*C7-C11	85,61	85,69	85,44	85,65
πC5-C9 →π^*C10-C12	88,20	88,03	84,98	80,88
πC7-C11→π^* C5-C9	72,15	72,11	72,61	72,69
πC7-C11→π^*C10-C12	83,68	84,60	84,19	85,82
πC10-C12 →π^*C5-C9	74,15	74,70	76,62	80,59
πC10-C12 →π^*C7-C11	73,32	73,07	73,90	74,32
$\Sigma_{\pi \rightarrow \pi^*}$	477,11	478,19	477,73	479,95
LP(1)N4→σ^*H29-Cl30			274,84	
$\Sigma_{LP \rightarrow \sigma^*}$			274,84	
LP(3)Br1→π^*C10-C12				41,97
LP(2)O2→π^*C7-C11	124,15	123,69	124,31	
$\Sigma_{LP \rightarrow \pi^*}$	124,15	123,69	124,31	41,97
π^*C7-C11→π^* C5-C9	844,49	875,33	1020,88	
π^*C10-C12 →π^* C5-C9	599,96	631,93	709,72	1024,56
$\Sigma_{\pi^* \rightarrow \pi^*}$	1444,44	1507,27	1730,60	1024,56
σN4-C8→LP*(1)H29				62,99
σN4-H21→LP*(1)H29				61,95
σN4-H22→LP*(1)H29				61,99
$\Sigma_{\sigma \rightarrow LP^*}$				186,93
LP(1)N4→LP*(1)H29				1584,64
LP(4)Cl30→LP*(1)H29				345,60
$\Sigma_{LP \rightarrow LP^*}$				1930,24
$\Sigma \Delta E_{TOTAL}$	2045.57	2109.15	2607.48	3663.65

[a]This work

Table 6 Main delocalization energies (in kJ/mol) for the cationic species of 2C-Bin gas phase by using B3LYP/6-31G* calculations.

Cationic Delocalization	Gas
$\pi C5\text{-}C7 \rightarrow \pi^* C9\text{-}C10$	45,19
$\pi C9\text{-}C10 \rightarrow \pi^* C11\text{-}C12$	45,19
$\pi C11\text{-}C12 \rightarrow \pi^* C5\text{-}C7$	44,27
$\Sigma_{\pi\rightarrow\pi^*}$	134,64
$LP(2)O2 \rightarrow \pi^* C7\text{-}C11$	56.01
$\Sigma_{LP\rightarrow\pi^*}$	56.01
$\pi^* C5\text{-}C7 \rightarrow \pi^* C9\text{-}C10$	118,17
$\pi^* C11\text{-}C12 \rightarrow \pi^* C9\text{-}C10$	111,2
$\Sigma_{\pi^*\rightarrow\pi^*}$	229,37
$\Sigma\Delta E_{TOTAL}$	420.02

[a]This work

Note that the latter transition is energetically the most strong in solution while the $n\rightarrow\pi^*$ transition presents the lower value in the same media. Analysing the transitions for the cationic species we observed that it species presents values very low, as compared with the other two species and, also only three transitions are observed: $\pi\rightarrow\pi^*$, $n\rightarrow\pi^*$ and $\pi^*\rightarrow\pi^*$. This study shows clearly that the hydrochloride species is the most stable of 2C-B in both media while the cationic ones is the less stable. This result is in complete concordance with the higher solvation energy observed for the cationic species despite with the 6-31G* basis set an imaginary frequency it is observed.

Atoms in Molecules (AIM) Studies

Bader has suggested from the Atoms in Molecules theory (AIM) that inter or intra-molecular, ionic, covalent or H bonds interactions can be easily predicted calculating the topological properties in the bond critical point (BCPs) or ring critical points (RCPs) [32]. Hence, the electron density, $\rho(r)$, the Laplacian values, $\nabla^2\rho(r)$, the eigenvalues $(\lambda 1, \lambda 2, \lambda 3)$ of the Hessian matrix and, the $|\lambda 1|/\lambda 3$ ratio have been computed for the three species of 2C-B with the AIM2000 program and the B3LYP/6-31G* method [33]. Thus, in Table 7 are summarized those properties for all species in gas phase and in aqueous solution while the molecular graphics for those three species are shown in Figures 7 and 8. The free base shows in gas phase a halogen H26---Br1 interaction not observed in solution while in the cationic species in gas phase the H26---Br1 and O2---H18 interactions are observed. These same interactions are observed in the hydrochloride species in gas phase but, both disappears in solution forming a new halogen H29---Cl30 interaction with characteristic ionic. Hence, when $\lambda 1/\lambda 3 < 1$ and $\nabla^2\rho(r) > 0$, for which, the interaction is ionic or highly polar covalent (closed-shell interaction).In Figure 8 can be seen the molecular graphic for the hydrochloride species in solution showing the interaction new formed. In this case, the distances between those two H and Cl atoms are closer than the other ones (2.009 Å).

The molecular graphics presented in Figure 7 evidence clearly all new interactions formed in each species of 2C-B. Here, the most important fact is that the ionic H29---Cl30 interaction observed in solution was not observed in gas phase because it presents covalent characteristics. Then, in the hydrochloride form in gas phase the H29-Cl30 has nature covalent while in solution the characteristic of this bond change to ionic. This fact is the most important result found by AIM studies. Other important result is that in the three species of 2C-B in gas phase,H and O atoms belonging to the two O-CH_3 groups participate in the formation of new interactions, as shown in Figures 7 and 8.

Table 7 Analyses of the topological properties in Bond Critical Points (BCPs) and Ring critical point (RCPs) for three species of 2 C-Bin gas phase and in aqueous solution by using the B3LYP/6-31G* method.

B3LYP/6-31G* Method					
Free base					
Parameter[#]	Gas phase				PCM
	H26---Br1	RCPN	RCP		RCP
ρ(r)	0.0081	0.0078	0.0196		0.0196
$\nabla^2\rho(r)$	0.0284	0.0326	0.1537		0.1534
λ1	-0.0057	-0.0044	-0.0141		-0.0141
λ2	-0.0039	0.0051	0.0766		0.0770
λ3	0.0380	0.0319	0.0912		0.0905
|λ1|/λ3	0.15	0.1379	0.1546		0.1558
Distances (Å)	2.943				
Cation gas					
Parameter[#]	H26---Br1	RCPN1	O2---H18	RCPN2	RCP
ρ(r)	0.0088	0.0082	0.0110	0.0099	0.0195
$\nabla^2\rho(r)$	0.0310	0.0351	0.0425	0.0474	0.1531
λ1	-0.0066	-0.0047	-0.0107	-0.0057	-0.0141
λ2	-0.0049	0.0064	-0.0075	0.0088	0.0765
λ3	0.0425	0.0333	0.0608	0.0442	0.0907
|λ1|/λ3	0.1553	0.1411	0.1760	0.1290	0.1555
Distances (Å)	2.889		2.450		
Hydrochloride					
Gas phase					
Parameter[#]	H26---Br1	RCPN1	O2---H18	RCPN2	RCP
ρ(r)	0.0081	0.0078	0.0080	0.0080	0.0196
$\nabla^2\rho(r)$	0.0283	0.0325	0.0328	0.0348	0.1537
λ1	-0.0057	-0.0044	-0.0066	-0.0056	-0.0141
λ2	-0.0038	0.0049	-0.0022	0.0025	0.0767
λ3	0.0379	0.0320	0.0417	0.0378	0.0911
|λ1|/λ3	0.1504	0.1375	0.1583	0.1481	0.1548
Distances (Å)	2.945		2.626		
PCM					
Parameter[#]	H29---Cl30	RCP			
ρ(r)	0.0434	0.0195			
$\nabla^2\rho(r)$	0.0746	0.1535			
λ1	-0.0567	-0.0141			
λ2	-0.0567	0.0771			
λ3	0.1880	0.0905			
|λ1|/λ3	0.3016	0.1558			
Distances (Å)	2.009				

[#] Ina.u.

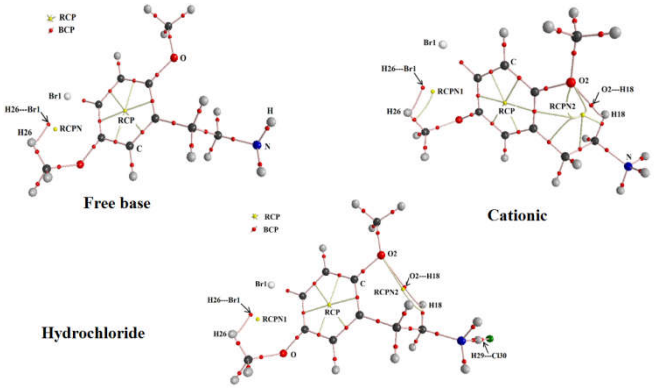

Figure 7 Molecular graphic for the free base, cationic and hydrochloride species of 2C-B in gas phase showing the geometry of all their bond critical points (BCPs) and ring critical points (RCPs) by using the B3LYP/6-31G* method.

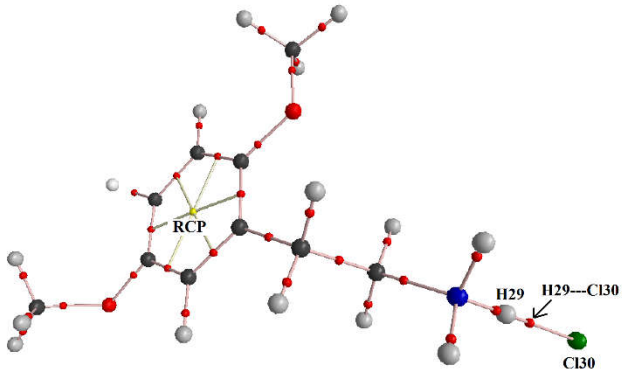

Figure 8 Molecular graphic for the hydrochloride species of 2C-B in aqueous solution showing the geometry of all their bond critical points (BCPs) and ring critical points (RCPs) by using the B3LYP/6-31G* method.

Frontier Orbitals and Quantum Global Descriptors Studies

The gap values for the three species of 2C-B in both media were calculated with the frontier orbitals, as recommended by Parr and Pearson [35] and, by using the hybrid B3LYP/6-31G* level of theory. Then, from known equations were later computed the chemical potential (μ), electronegativity (χ), global hardness (η), global softness (S), global electrophilicity index (ω) and global nucleophilicity index (E) descriptors [36-41] in order to predict the reactivities and behaviours of those three species. Thus, these properties are presented in Table 8 together with the equations used to calculate the descriptors. The gap values clearly evidence that the hydrochloride species in solution is the most reactive than the other ones, and later, the cationic species. Comparing these gap values with values for other species in Table 9 we observed that cocaine in both media present the lower values which are similar to the observed for the hydrochloride species of 2C-B. Hence, cocaine is the most reactive species in both media.

Table 8 Frontier molecular HOMO and LUMO orbitals and some descriptors for the three species of 2C-B in gas phase and in aqueous solution by using the B3LYP/6-31G* method.

B3LYP/6-31G* method[a]						
Orbitals	**Free base**		**Cationic**		**Hydrochloride**	
(eV)	**Gas**	**PCM**	**Gas**	**PCM**	**Gas**	**PCM**
HOMO	-5.7824	-5.8205	-8.7430		-6.1715	-4.9117
LUMO	-0.3211	-0.3401	-4.3375		-0.6585	-1.0939
|GAP|	5.4613	5.4804	4.4055		5.5130	3.8178
DESCRIPTORS						
(eV)	**Gas**	**PCM**	**Gas**	**PCM**		
χ	-2.7307	-2.7402	-2.2028		-2.7565	-1.9089
μ	-3.0518	-3.0803	-6.5403		-3.4150	-3.0028
η	2.7307	2.7402	2.2028		2.7565	1.9089
S	0.1831	0.1825	0.2270		0.1814	0.2619
ω	1.7053	1.7313	9.7094		2.1154	2.3618
E	-8.3333	-8.4406	-14.4065		-9.4134	-5.7320

[a]Thiswork

$\chi = -[E(LUMO) - E(HOMO)]/2$; $\mu = [E(LUMO) + E(HOMO)]/2$; $\eta = [E(LUMO) - E(HOMO)]/2$;
$S = \frac{1}{2}\eta$; $\omega = \mu^2/2\eta$ E=mu

Table 9 Gap values for the three species of 2C-B compared with other species in gas and aqueous solution phases by using the B3LYP/6-31G* level of theory.

Free base/Gas phase								
Orbital	**Scopolamine[#,b]**	**Heroin[c]**	**Morphine[d]**	**Cocaine[e]**	**Tropane[f]**	**Cyclizine[g]**	**Promethazine[h]**	
							S(-)	**R(+)**
|GAP|	5.4004	5.6563	5.6044	4.8580	7.5506	5.3946	4.7157	4.7756
Free base/Aqueous solution								
|GAP|	5.4758	5.6414	5.4750	4.9487	7.6611	5.5067	4.7702	4.8028
Cationic/Gas phase								
|GAP|	5.6356	5.4268	5.1889	5.4468	9.5595	5.5823	4.5661	4.5770
Hydrochloride/Gas phase								
|GAP|	4.9239	5.3024	5.4417	3.6813	6.8246		4.8654	4.8110
Hydrochloride/Aqueous solution								
|GAP|	5.4026	4.4469	4.5840	3.6813	5.9119	4.2159	4.2042	4.4926

[#]Hydrobromide, [a]This work, [b]From Ref [19], [c]From Ref [17],[d]From Ref [13],[e]From Ref [15],[f]From Ref [14],[g]From Ref [21], [h]From Ref [22]

Analysing the descriptors, the cationic species in gas phase present the highest global electrophilicity and nucleophilicity indexes than the other ones, a result similar to observed in the two enantiomer of promethazine [22]. Moreover, the cationic species of 2C-B has a global electrophilicity index (ω) higher than scopolamine, heroin, morphine, cocaine, tropane, cyclizine and the two S(-) and R(+) forms of promethazine [13-22]. In relation to nucleophilicity index (E) value, the value observed for the cationic species of 2C-B (-14.4065 eV) is higher than the two forms of promethazine (-12.9219 and-12.9341 eV) but lower than the values of scopolamine (-16.9925 eV), heroin (-16.4174 eV), morphine (-15.4288 eV), cocaine (-17.9548 eV)and cyclizine (-16.8238 eV). Here, probably the high E value observed for this species could justify the similar solvation energy, as compared with morphine and cocaine.

Vibrational Study

The structures each species of 2C-B were optimized with C_1 symmetries by using the hybrid B3LYP/6-31G* method and, for free base, cationic and hydrochloride species are expected 78, 81 and 84 normal vibration modes, respectively. The experimental available attenuated total reflectance (ATR) and Raman spectra of hydrochloride species of 2C-Bin solid phase can be observed in Figures 9 and 10 respectively compared with the corresponding predicted for the three species in gas phase. In this work, the ATR spectrum was taken from [47] while the Raman spectrum between 1700 and 400 $cm^{-1}$was taken from Ref [12].The predicted Raman spectra in activities were changed to intensities by using equations reported in the literature [45,46].

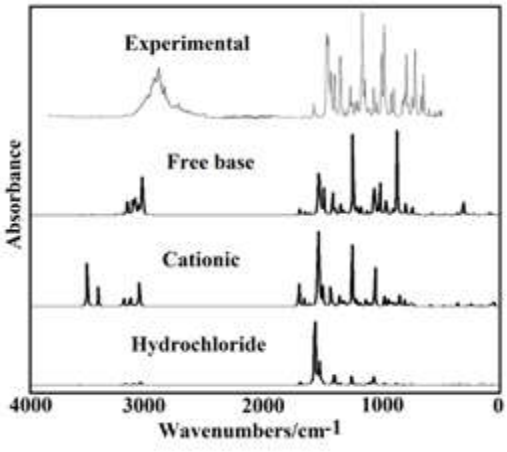

Figure 9 Experimental infrared spectrum of 2C-B in the solid state [47] compared with the corresponding predicted for free base, cationic and hydrochloride species by using the B3LYP/6-31G* method.

Table 10 Observed and calculated wavenumbers (cm-1) and assignments for the three species of 2C-B in gas and in aqueous solution phases.

Experimental			B3LYP/6-31G* Method[a]					
			Free base GAS		Cationic GAS		HClgas	
IR[c]	ATR[c]	Raman[d]	SQM[b]	Assignments[a]	SQM[b]	Assignments[a]	SQM[b]	Assignments[a]
			3391	ν_aNH_2	3344	ν_aNH_3	3405	ν_aNH_3
	3195w		3310	ν_sNH_2	3340	ν_aNH_3	3324	ν_sNH_3,ν_aNH_3
					3252	ν_sNH_3		
			3112	νC11-H20	3115	νC11-H20	3115	νC11-H20
			3063	νC9-H19	3068	νC9-H19	3065	νC9-H19
					3062	ν_aCH_2(C8)		
					3045	ν_aCH_3(C14)	3033	ν_aCH_3(C13)
3002sh			3029	ν_aCH_3(C13)	3041	ν_aCH_3(C13)	3027	ν_aCH_3(C14)
3000w			3023	ν_aCH_3(C14)	2996	ν_sCH_2(C8)	3014	ν_aCH_2(C8)
2983sh	2987w		2983	ν_aCH_2(C8)	2994	ν_aCH_3(C13)	2975	ν_aCH_3(C14)
			2972	ν_aCH_3(C14)	2994	ν_aCH_3(C14)	2968	ν_aCH_3(C13)
2963sh			2961	ν_aCH_3(C13)	2965	ν_aCH_2(C6)	2963	ν_sCH_2(C8)
			2953	ν_aCH_2(C6)			2953	ν_aCH_2(C6)
2943m			2932	ν_sCH_2(C8)	2925	ν_sCH_3(C13)		
2910sh	2919m		2912	ν_sCH_2(C6)	2921	ν_sCH_3(C14)	2915	ν_sCH_2(C6)
2895sh	2880m		2906	ν_sCH_3(C14)	2915	ν_sCH_2(C6)	2908	ν_sCH_3(C13)
2840w	2819m		2903	ν_sCH_3(C13)			2907	ν_sCH_3(C14)
1603w	1600w	1585m	1645	δNH$_2$	1624	δ_aNH_3	1612	δ_aNH_3
	1573w		1599	νC5-C9 νC9-C10	1619	δ_aNH_3	1601	νC5-C9
		1562w	1562	νC5-C7 νC10-C12 νC7-C11	1601 1559	νC5-C9 νC5-C7νC10-C12	1562	νC5-C7 νC10-C12
1498vs	1496vs		1491	βC9-H19			1503	νH29-Cl30
1488sh	1483vs				1489	βC11-H20	1490	βC11-H20 βC9-H19
1472sh			1468	δ_aCH_3(C13)	1468	δ_aCH_3(C13)		
					1465	δ_aCH_3(C14)	1467	δ_aCH_3(C14)
	1461m		1467	δ_aCH_3(C14)	1465	δ_sNH_3	1467	δ_aCH_3(C13)
		1458w	1458	δCH$_2$(C8)	1459	δCH$_2$(C8)	1456	δCH$_2$(C8)
			1455	δ_aCH_3(C13)	1454	δ_aCH_3(C13)	1455	δ_aCH_3(C13)
			1452	δ_aCH_3(C14)	1453	δ_aCH_3(C14)	1452	δ_aCH_3(C14)
1440sh		1441w	1442	δCH$_2$(C6)	1437	δCH$_2$(C6)	1440	δCH$_2$(C6)
	1433m		1435	δ_sCH_3(C13)	1436	δ_sCH_3(C14)	1435	δ_sCH_3(C14)
1420w		1420w	1434	δ_sCH_3(C14)	1433	δ_sCH_3(C13)	1433	δ_sCH_3(C13)
	1386s		1385	wagCH$_2$(C8)	1391	wagCH$_2$(C8)	1385	wagCH$_2$(C8)
1375w	1373sh	1374w	1376	νC5-C9 νC11-C12	1380	wagCH$_2$(C8) νC11-C12	1375	wagCH$_2$(C8)
	1342w		1365	ρCH$_2$(C8) ρNH$_2$	1327	wagCH$_2$(C6)	1347	ρCH$_2$(C8)
	1312sh	1313w	1309	wagCH$_2$(C6) νC10-C12	1317	ρCH$_2$(C8)	1316	wagCH$_2$(C6)
	1303m	1296w	1304	wagCH$_2$(C6)	1289	νC7-C11νC9-C10	1303	νC7-C11 νC9-C10
1275w	1289w	1280s	1273	νO3-C10	1270	νO3-C10νC11-C12	1270	νO3-C10
	1261w	1259w	1260	νC11-C12	1259	βC9-H19	1260	νC11-C12
1230sh	1245w	1235w	1243	βC11-H20	1231	ρCH$_2$(C6)	1238	βC11-H20
1218vs	1220sh		1216	νO2-C7	1209	νO2-C7ρCH$_3$(C14)	1214	νO2-C7
1199sh	1207vs	1200vw	1188	ρCH$_3$(C14)	1184	ρCH$_3$(C13)	1187	ρCH$_3$(C14)
1177sh	1199sh	1186w	1187	ρCH$_3$(C13)	1183	ρCH$_3$(C14)	1185	ρCH$_3$(C13)
1152sh	1182m		1154	ρ'CH$_3$(C13)	1151	ρ'CH$_3$(C13)	1153	ρ'CH$_3$(C13)
1152sh	1155w	1147w	1154	ρ'CH$_3$(C14)	1151	ρ'CH$_3$(C14)	1153	ρ'CH$_3$(C14)
	1122sh		1149	νC5-C6	1146	νC5-C6βR_1(A1)	1148	νC5-C6 βC9-H19
1104w	1115m		1100	ρCH$_2$(C6)				
	1090w	1086w			1090	νC6-C8 ρNH$_3$	1092	ρCH$_2$(C6)ρ'NH$_3$
1066sh	1052s		1060	νC8-N4			1066	δ_aNH_3
1047m		1044w	1042	νO2-C13 βR_1(A1)	1036	ρ'NH$_3$νO3-C14	1038	νO2-C13 βR_1(A1)
							1034	νC8-N4
1027sh	1027s	1019w	1029	νO3-C14	1027	νO2-C13	1028	νO3-C14
1001sh			990	νC6-C8	1016	νO3-C14	1010	νC6-C8
	973w	963w					975	τN4-H29
943vw	948m	946m	946	νO3-C14 νC5-C6	946	νO3-C14	945	νO3-C14 νC5-C6
915vw		930sh	910	γC9-H19	911	γC9-H19	907	γC9-H19
			903	γC9-H19	898	νC6-C8γC9-H19		
	877w				882	γC11-H20	872	τwCH$_2$(C6)
864w	863w		867	γC11-H20	854	ρ'NH$_3$	869	γC11-H20
841w	846s				821	νC8-N4	839	δN4H29Cl30
789m	800w	797m	797	wagNH$_2$	781	νO2-C7	785	νO2-C7 νC5-C7
	777s		778	wagNH$_2$δNH$_2$				
		732w	739	γC10-O3	741	γC10-O3	740	γC10-O3
	727w		729	τR_1(A1)γC7-O2	722	τR_1(A1)	729	τR_1(A1)
	709m	712vs	699	τwCH$_2$(C8) τwCH$_2$(C6)	706	τwCH$_2$(C8) τwCH$_2$(C6)	701	τwCH$_2$(C8)
	663w	665w	691	τR_3(A1) γC10-O3	689	τR_3(A1)γC7-O2	691	τR_3(A1) γC7-O2
	620w	632w	627	βR_2(A1)	629	γC7-O2τR_3(A1)	629	βR_2(A1)
	577w	614w	577	βC10-O3 βC7-O2	577	βC10-O3 βC7-O2	576	βC10-O3 βC7-O2
	562w	493m	517	βR_3(A1)	516	γC12-Br1βR_3(A1)	518	βR_3(A1)
		474sh	471	τR_2(A1) γC7-O2γC5-C6	465	τR_2(A1)	471	τR_2(A1) γC7-O2γC5-C6
		432sh	462	γC12-Br1	462	γC7-O2	462	γC12-Br1

				366	δC13O2C7
360	δC13O2C7	356	δC13O2C7	361	$\delta_a NH_3$
321	τR_1(A1)			334	$\nu_a NH_3 \nu_s NH_3$
295	βC5-C6	307	δC6C8N4	289	βC5-C6
279	$\tau_w NH_2$	276	βC5-C6		
259	τwCH_3(C13)	254	τwCH_3(C13)	259	$\nu_a NH_3 \nu_s NH_3$
248	βR_2(A1) νC12-Br1	246	βR_2(A1)	256	τwCH_3(C13)
227	νC12-Br1	224	νC12-Br1	226	νC12-Br1 βC12-Br1
205	δC14O3C10	203	τwCH_3(C13) τwNH_3	202	δC14O3C10
		199	τwNH_3		
166	δC5C6C8	167	δC5C6C8	170	δC5C6C8
157	τwCH_3(C14)	155	βC12-Br1	156	τwCH_3(C14)
147	βC12-Br1			147	$\nu_s NH_3$
		142	τwCH_3(C14)	145	$\nu_a NH_3 \nu_s NH_3$
127	τ_wO2-C7 τR_2(A1)	132	τ_wO2-C7τR_3(A1)	127	τ_wO2-C7 τR_2(A1)
87	τC8-C6	92	τ_wO3-C10	89	τ_wC6-C5
85	τ_wO3-C10	85	τC8-C6τ_wC6-C5	86	τ_wO3-C10
67	τ_wO2-C7	72	τ_wO2-C7	68	τ_wO2-C7
50	τ_wC6-C5	53	τR_3(A1)	60	τC8-C6
45	τR_3(A1)	45	γC5-C6	47	τR_3(A1)
				22	ρNH_3
				16	τwNH_3

Abbreviations: ν, stretching; β, deformation in the plane; γ, deformation out of plane; wag, wagging; τ ,torsion; β_R, deformation ring τ_R, torsion ring; ρ, rocking; τw, twisting; δ, deformation; a, antisymmetric; s, symmetric; (A_1), Ring 1; [a]This work, [b]From scaled quantum mechanics force field, [c]From Ref [47], [d]From Ref [12].

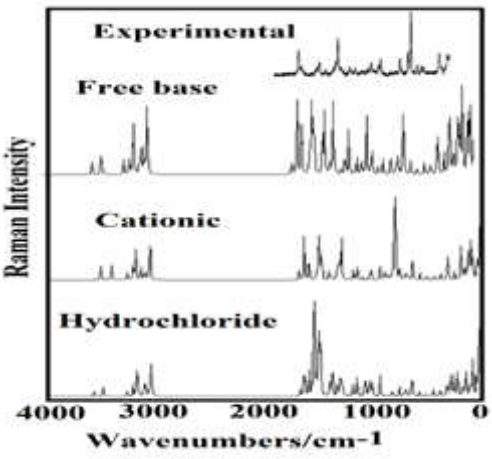

Figure 10 Experimental Raman spectrum of 2C-B in the solid state [12] compared with the corresponding predicted for free base, cationic and hydrochloride species by using the B3LYP/6-31G* method

Both spectra show better correlations for the cationic species because the hydrochloride species in solution presents the ionic H29---Cl30 bond, as evidenced by AIM calculations while the free base in this medium is protonated forming the cationic species. The normal internal coordinates of each species were employed together with the corresponding harmonic force fields calculated by using the SQMFF approach [42] and the Molvib program [44]to perform the complete vibrational study. Here, potential energy distribution (PED) contributions higher or equal to 10% were used in the assignments of the bands observed in both spectra. In Table 10 are presented the observed and calculated wavenumbers and assignments for the three species of 2C-B in gas phase and in aqueous solution. The experimental available IR bands presented in Table 10 were taken from Ref [47] for the hydrochloride species of 2C-B in vapor phase.Later, short discussions of some assignments are presented at continuation.

Band Assignments

NH_2 modes: The antisymmetrical and symmetrical modes of these groups are expected only for the free base of 2C-B.

Thus, taking into account that both modes are predicted by SQM calculations at 3391 and 3310 cm^{-1} the ATR band at 3195 $cm^{-1}$is assigned to both modes, as in similar compounds [38,50]. Note that due to the absence of Raman bands in this region the symmetries of these modes wereonly predicted but not identified. The NH_2 deformation mode is predicted at 1645 cm^{-1} while the expected rocking, waging and twisting modes are predicted respectively in the 1365, 797/778 and 279 cm^{-1}region. Consequently, these modes are assigned to the IR, ATR and Raman bands observed in those regions.

NH_3 modes: These modes are expected only for the cationic and hydrochloride species of 2C-B. The two NH_3 antisymmetric and symmetric stretching modesin zwitterionic species of some compounds are assigned between 3207 and 3106 cm^{-1}[51-55]. Here, in the cationic and hydrochloride species these modes are predicted at 3344/3340 and 3405/3324 cm^{-1}, respectively. Thus, these modes are related with the ATR band at 3195 cm^{-1}.The antisymmetric and symmetric NH_3 deformation modes in the cationic species are predicted at 1624, 1619 and 1465cm^{-1} while those modes in the hydrochloride species are predicted at 1612, 361 and 1066 cm^{1}, respectively. The ionic H29---Cl30 bond linked to the N4-H29 bond justifies that low value predicted for one of the two antisymmetric modes. These same reasons could justify that the two rocking and twisting modes appear in the hydrochloride species in different regions. In the cationic species the two rocking modes are predicted at 1036 and 854 cm^{-1} and the twisting mode at 199 cm^{-1}while in the hydrochloride species the two rocking modes are predicted at 1092 and 22 cm^{-1} and the twisting mode at 16 cm^{-1}. Hence, the vibration modes predicted in the 400-10 cm^{-1} region could not be assigned because the vibrational spectra were not recorded in this region.

CH modes. In the three species of 2C-B only the vibration modes corresponding to the two aromatics C9-H19 and C11-H20 bonds belonging to the phenyl ring are expected. In the three species, the SQ Mcalculations predicted the C9-H19 stretching modes at higher wavenumbers than the other ones due probably to the proximities of C11-H20 bonds with the Br atoms, hence, the weak and broad ATR band at 3195 cm^{-1}can also be associated to these vibration modes. In other species and, in particular in dimer species, these modes are assigned between 3163 and 3069 cm^{-1}[56-58]. Generally, the in-plane

deformation or rocking modes are assigned between 1377 and 1157 cm^{-1}[56-58], hence, these modes in the three species can be assigned in this region, as detailed in Table 10. The out-of-phase modes associated with those two bonds in the three species of 2C-B can be assigned in accordance with the calculations between 910 and 867 cm^{-1}.

***CH_3 modes*:** In the three species of 2C-B there are two CH_3 groups that belong to the O-CH_3groups. In species containing this group, the antisymmetric and symmetric stretching modes are normally assigned in the 3090-2914 cm^{-1} region [13-15,17-22,37,39,40,50,54,56-58]. Here, these modes are predicted between 3045 and 2903 cm^{-1}, for which, they are assigned accordingly. Evidently, the symmetries of these modes were not determined because the Raman spectrum was recorded between 1700 and 400 cm^{-1}. The CH_3 deformation, rocking and twisting modes are assigned as predicted by SQM calculations performed here and, in accordance to similar species [13-15,17-22,37,39,40,50,54,56-58].

CH_2 Modes: The species of 2C-B present two CH_2 groups, for which, four antisymmetrical and symmetric modes are expected and, also the deformation, rocking, waging and twisting modes. All these modes are predicted and assigned at 3062/2925, 1459/1437, 1391/1304, 1365/1092 and 872/699 cm^{-1},respectively. These vibration modes in compound containing these CH_2 groups are assigned in approximately the same regions [13-15,17-22,37,39,40,50,54,56-58].

Skeletal Modes: In compounds that present the C-O bond, as in carquejol [56], the C-O stretching modes are assigned to 1065 cm^{-1}. Here, in the species of 2C-B are expected four C-O stretching, where two of them belong to O-CH_3 groups and the other two are linked to the phenyl rings. The SQM calculations predicted the two C-O stretching modes linked to the rings at higher wavenumbers (1273 and 1209 cm^{-1}) than other ones (1028 and 945 cm^{-1}), hence, they are easily assigned to the strong and very strong IR, ATR and Raman bands observed in those regions. Note that the strong ATR band at 1052 cm^{-1}can be assigned to the C8-N4 stretching modes or to the symmetrical deformation modes of hydrochloride species, as indicated Table 10. The C=C stretching modes are predicted in the expected regions, in accordance with similar compounds and assigned, accordingly [13-15,17-22,37,39,40,50,54,56-58]. The assignments of remaining skeletal modes only were assigned up to 400 cm^{-1} while from 400 up to 10 $cm^{-1}$the vibration modes were not assigned because the experimental vibrational spectra were only recorded up to 400 cm^{-1}.

Force Fields

The AIM studies have evidenced that the cationic and hydrochloride species present practically the same interactions and stabilities in gas phase but the H29-Cl30 bonds in both species show different characteristics, hence, in order to investigate the force of these bonds the harmonic force constants were calculated for the three species of 2C-B in both media. Therefore, the force constants determined from the corresponding harmonic force fields at the 6-31G* level of theory with the SQMFF methodology [25] and the Molvib program [37] are summarized in Table 11.First, the comparisons of *f(νN-H)* force constants for the three species show that the hydrochloride species presents low values in both media, as compared with the other two species. These differences can be attributed to the different characteristics of H29-Cl30 bonds because in the hydrochloride species this bond is linked to N4-H29 bond that belong to NH_3^+ group. Obviously, in this species that bond is different from the other two N-H bonds.The presence of Cl atom in the hydrochloride species generates changes significant in the *f(νC-N)*force constants values in both media but lower changes are observed in the $f(\nu CH_2)$,$f(\nu CH_3)$ and*f(νC-Br)*force constants.The free base of 2C-B shows high *f(νN-H)* force constant values in both media, in relation to the cationic and hydrochloride species because the NH_2 group has practically the two N-H bonds equivalents.

Table 11 Scaled internal force constants for the free base, cationic and hydrochloride species of 2C-b in gasphase and in aqueous solution by using the B3LYP/6-31G* method.

Forceconstants	2C-B[a]				
	Free base		Cationic	Hydrochloride	
	Gas	PCM	Gas	Gas	PCM
$f(\nu N\text{-}H)$	6.24	6.18	6.10	4.35	5.62
$f(\nu C\text{-}N)$	3.59	3.72	3.16	4.50	4.13
$f(\nu CH_2)$	4.79	4.81	4.91	4.84	4.93
$f(\nu CH_3)$	4.76	4.91	4.92	4.86	4.92
$f(\nu C\text{-}H)_R$	5.24	5.26	5.25	5.24	5.27
$f(\nu C\text{-}O)_R$	5.41	5.07	5.25	5.40	5.10
$f(\nu C\text{-}O)_{OCH3}$	5.26	4.99	5.30	5.26	4.99
$f(\nu C\text{-}Br)$	2.72	2.65	2.87	2.74	2.70
$f(\delta CH_2)$	0.78	0.77	0.78	0.78	0.77
$f(\delta CH_3)$	0.59	0.58	0.58	0.59	0.58

Units are mdyn $Å^{-1}$ for stretching and mdyn Å rad^{-2} for angle deformations

[a]This work

This force constant in solution decrease its value as a consequence of hydration of these bonds with water molecules. In the free base and hydrochloride species the $f(\nu C\text{-}O)_R$ force constant spresent higher values in both media than the $f(\nu C\text{-}O)_{OCH3}$ force constants while in the cationic species a different result is obtained in gas phase. Hence, these changes of those two constants in solution evidence the hydration of both O-CH_3 group**s** with water molecules.

Ultraviolet-visible spectrum

The experimental available UV-visible spectrum of 2C-B was taken from Ref [11] and it is compared with those predicted for free base and hydrochloride species in aqueous solution by using TD-DFT calculations with the B3LYP/6-31G* method and the Gaussian program [24]. These spectra are compared in Figure 11. The experimental spectrum shows a maximum at 393 nm with a shoulder between 215 and 230 nm while in the predicted spectrum of free base is observed a maximum at 199 nm and a shoulder at 240 nm. In the predicted spectrum of hydrochloride species is observed a maximum at 314.5 nm. Here, the cationic species is clearly observed in aqueous solution because in this medium the free base is protonated while the hydrochloride species is present as cationic one. Thus, in the experimental UV-vis spectrum only can be seen a band and a shoulder because it was recorded from 200 up to 400 nm. Here, these bands could be associated to$\pi \rightarrow \pi^*$ transitions due to C=C double bonds of phenyl ring, as predicted the NBO calculations and in agreement with similar compounds [56-58].

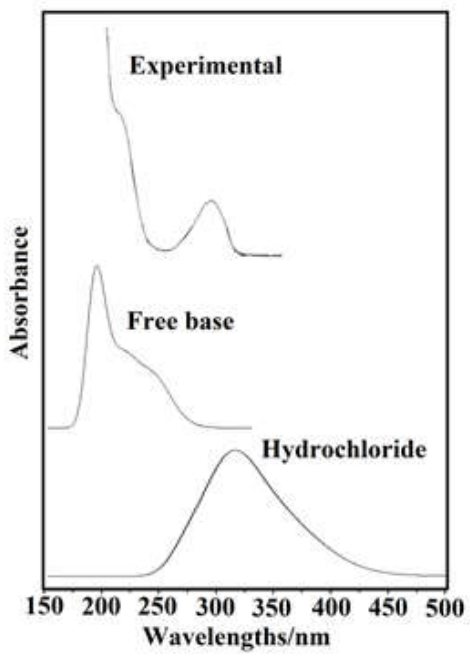

Figure 11. Experimental UV-visible spectrum of 2C-B compared with the corresponding predicted for the free base and hydrochloride species by using B3LYP/6-31G* frequencies.

NMR study

In Tables 12 and 13 are presented the experimental available ^{1}H and ^{13}C NMR chemical shifts of 2C-B in D_2O and $CDCl_3$ from Ref [11,47], respectively which are compared with the corresponding predicted in aqueous solution by using the GIAO [39] and the B3LYP/6-31G* methodsby means of the RMSD values. For some nucleus the values are overestimated in relation to the experimental ones, hence, for the ^{1}H nucleus (1.7-1.1 ppm) it is observed a better concordance while for the ^{13}C nucleus the RMSD values slightly increase for the two comparisons. Thus, when the values are compared with the values taken from Ref [47] the RMSD values are about 8.7 and 9.0 ppm and, when the values from Ref [11] are considered the RMSD values increase notably up to 11.9 and 10.4 ppm. These differences can be quickly justified by the calculations because the 6-31G* basis set was employed instead of that recommended 6-311++G** basis set. Besides, the two H atoms of NH_2 group in the free base were predicted by calculations with negative values, as can be seen in Table 12.

Table 12 Observed and calculated ^{1}H chemical shifts (δ in ppm) for the three forms of 2C-B in gas phase and in aqueous solution by using the B3LYP/6-31G* method.

δ (ppm)	B3LYP/631G* Method		Exp[b]
	Free base	Hydrochloride	
15-H	1.63	1.68	3.77
16-H	2.42	2.47	3.77
17-H	2.15	2.50	3.82
18-H	2.58	2.83	3.82
19-H	6.40	6.42	6.90
20-H	6.00	6.17	7.50
21-H	-0.17	2.01	3.55
22-H	-0.11	2.11	3.55
23-H	3.20	3.38	2.91
24-H	3.62	3.68	2.91
25-H	3.18	3.19	2.91
26-H	3.50	3.57	3.20
27-H	2.92	2.91	3.20
28-H	3.42	3.52	3.20
RMSD[b]	**1.7**	**1.1**	

[a]This work, [b]From Ref [47] in D2O

Table 13 Observed and calculated ^{13}C chemical shifts (δ in ppm) for the three forms of 2C-B in gas phase and in aqueous solution by using the B3LYP/6-31G* method.

δ (ppm)	B3LYP 631G* Method[a]		Exp[b]	Exp[c]
	Free base	Hydrochloride		
5-C	115.29	108.38	118.00	128,11
6-C	34.59	25.50	30.00	30,53
7-C	139.38	139.16	154.00	154,90
8-C	37.62	33.31	40.50	42,15
9-C	113.27	113.74	117.00	118,47
10-C	137.45	138.13	152.00	152,13
11-C	101.41	102.77	112.00	119,33
12-C	120.58	124.87	126.00	112,46
13-C	46.24	46.60	57.00	42,15
14-C	52.46	52.44	58.00	52,73
RMSD[b]	**8.7**	**9.0**		
RMSD[c]	**10.4**	**11.9**		

[a]This work, [b]From Ref [47]in CD_3OD, [c]From Ref [11]

CONCLUSIONS

In the present work, the molecular structures of free base, cationic and hydrochloride species of potent psychotropic 4-Bromo-2,5-dimethoxyphenethylamine (2C-B) drug were theoretically determined in gas phase and in aqueous solution by using hybrid B3LYP/6-31G* method. Then, the structural, electronic, topological and vibrational properties of have been evaluated by using the same level of theory while the experimental available infrared, attenuated total reflectance (ATR), Raman, ^{1}H-, ^{13}C-NMR and ultraviolet-visible spectroscopies were compared with the corresponding predicted at the same level of theory. In solution, the properties for those three species were predicted at the same level of theory by using the polarized continuum (PCM) and the universal solvation model. The cationic species of 2C-B shows higher solvation energy than the other ones, presenting values approximately similar to those observed for morphine, scopolamine and heroin alkaloids. NBO calculations suggest that hydrochloride species is most stable in solution while the AIM studies reveal that in the hydrochloride species in gas phase the H29-Cl30 bond has nature covalent while in solution change to ionic. The studies by using the frontier orbitals have evidenced that the gap value for the hydrochloride species in solution is similar to that observed for cocaine. The cationic species of 2C-B has a global electrophilicity index higher than scopolamine, heroin, morphine, cocaine, tropane, cyclizine and the two S(-) and R(+) forms of promethazine. A very important difference of three species of 2C-B with the tropane alkaloids is that the hydrochloride species in 2C-B is linked to N-H of NH_3^+ groups while in the alkaloids to N-H of quaternary amine. The complete assignments of expected78, 81 and 84 normal vibration modes for free base, cationic and hydrochloride species of 2C-B are performed with the corresponding harmonic force fields by using the scaled quantum mechanical force field (SQMFF) methodology. The force constants are also reported. The bands observed in the predicted UV-Vis spectra for the free base and hydrochloride species evidence that the cationic species is clearly present in solution, as compared with the experimental ones.

Acknowledgements

This work was supported with grants from CIUNT Project Nº 26/D608 (Consejo de Investigaciones, Universidad Nacional

de Tucumán).The authors would like to thank Prof. Tom Sundius for his permission to use MOLVIB.

References

1. PapaseitE, FarréM, Pérez-MañáC, TorrensM, VenturaM, PujadasM, de la TorreR, GonzálezD.Acute Pharmacological Effects of 2C-B in Humans: An Observational Study. Frontiers in Pharmacology, 2018, 9(206): 1-10.
2. Tracy DK., Wood DM, Baumeister D. Novel psychoactive substances: types, mechanisms of action, and effects. BMJ,2017, 356:i6848. doi: 10.1136/bmj.i6848.
3. Kanamori T, Yamamuro T, Kuwayama K, Tsujikawa K, Iwata YT, Inoue H. Synthesis and analysis of glucuronic acid-conjugated metabolites of 4-Bromo-2,5-dimethoxyphenethylamine, J. Forensic Sci.,2017, 62: 488–492. doi: 10.1111/1556-4029.13266.
4. Caicedo J, Berrouet MC, Saldarriaga JC. The risk of 2, 5-dimethoxy-4-bromophenylethylamine (2C-B): case. Med. UPB,2016, 35:139–143.doi: 10.18566/medupb.v35n2.a08.
5. González D, Torrens M, Farré M. Acute effects of the novel psychoactive drug 2C-B on emotions. Biomed. Res. Int., 2015, 2015:643878. doi: 10.1155/2015/643878.
6. Papoutsis I, Nikolaou P, Stefanidou M, Spiliopoulou C, Athanaselis S. 25B-NBOMe and its precursor 2C-B: modern trends and hidden Dangers. Forensic Toxicol., 2015,33: 1–11. doi: 10.1007/s11419-014-0242-9.
7. Nugteren-van Lonkhuyzen JJ, van Riel AJ, Brunt TM, Hondebrink L. Pharmacokinetics, pharmacodynamics and toxicology of new psychoactive substances (NPS): 2C-B, 4-fluoroamphetamine and benzofurans. Drug Alcohol Depend, 2015, 157: 18–27. doi: 10.1016/j.drugalcdep.2015.10.011.
8. TheobaldDS, FritschiG, Maurer HH. Studies on the toxicological detection of the designer drug 4-bromo-2,5-dimethoxybeta-phenethylamine (2C-B) in rat urine using gas chromatography-mass spectrometry. J. Chromatogr. B Analyt. Technol. Biomed. Life Sci.,2007, 846: 374–377. doi: 10.1016/j.jchromb.2006.08.049.
9. Ferreira da Costa Ferreira Carmo, HM. Estudo Da Influência Do Metabolismo NaToxicidade De Derivados Anfetaminicos: 4-MTA, 2C-B e MDMA, Doctoral Thesis, University of Porto, 2007.
10. Villalobos CA, Bull P, Sáez P, Cassels BK, Huidobro-Toro JP. 4-Bromo-2,5-dimethoxyphenethylamine (2C-B) and structurally related phenylethylamines are potent 5-HT2A receptor antagonists in Xenopuslaevis oocytes. Br. J. Pharmacol., 2004,141: 1167–1174. doi: 10.1038/sj.bjp.0705722
11. GiroudC, AugsburgerM, RivierL, P. Mangin, SadeghipourF, VaresioE,. VeutheyJL, KamalaprijaP. 2C-B: A New Psychoactive Phenylethylamine Recently Discovered in Ecstasy Tablets Sold on the Swiss Black Market. Journal of Analytical Toxicology, 1998, 22: 345-354.
12. BellSEJ., BurnsDT, DennisAC, SpeersJS. Rapid analysis of ecstasy and related phenethylamines in seized tablets by Raman spectroscopy. Analyst, 2000, 125: 541–544.
13. BrandánSA. Why morphine is a molecule chemically powerful. Their comparison with cocaine.Indian Journal of Applied Research, 2017,7(7): 511-528.
14. RudykR., BrandánSA. Force field, internal coordinates and vibrational study of alkaloid tropane hydrochloride by using their infrared spectrum and DFT calculations. Paripex A Indian Journal of Research, 2017,6(8): 616-623.
15. RomaniD, BrandánSA. Vibrational analyses of alkaloid cocaine as free base, cationic and hydrochloride species based on their internal coordinates and force fields. Paripex A Indian Journal of Research, 2017.6(9): 587-602.
16. Iramain MA, Ledesma AE, BrandánSA.Analyzing the effects of halogen on properties of a halogenated series of R and S enantiomers analogues alkaloid cocaine-X, X=F, Cl, Br, I. Paripex A Indian Journal of Research, 2017,6(12): 454-463.
17. Brandán SA.Understanding the potency of heroin against to morphine and cocaine. IJSRM, International Journal of Science and Research Methodology, 2018, 12(2): 97-140.
18. Rudyk RA, Checa MA, Guzzetti KA, Iramain MA, Brandán SA. Behaviour of N-CH_3 Group in Tropane Alkaloids and correlations in their Properties.IJSRM, International Journal of Science And Research Methodology, 2018; 10 (4): 70-97.
19. Rudyk RA,Checa MA, Catalán CAN, Brandán SA.Structural, FT-IR, FT-Raman and ECD spectroscopic studies of free base, cationic and hydrobromide species of scopolamine alkaloid. J. Mol. Struct. , 2019, 1180: 603-617..
20. IramainMA, BrandánSA. Structural and vibrational properties of three species of anti-histaminic diphenhydramine by using DFT calculations and the SQM approach. Journal: To Chemistry Journal, 2018,1(1): 105-130.
21. MárquezMJ, Iramain MA, BrandánSA.*Ab-initio* and Vibrational studies on Free Base, Cationic and Hydrochloride Species Derived from Antihistaminic Cyclizine agent.IJSRM, International Journal of Science and Research Methodology,2018, 12(2): 97-140.
22. ManzurME, BrandánSA.S(-) and R(+) Species Derived from Antihistaminic Promethazine Agent: Structural and Vibrational Studies, Submitted to Heliyon (2019).
23. NielsenAB, HolderAJ. Gauss View 3.0. User's Reference, GAUSSIAN Inc., Pittsburgh, PA, 2000–2003.
24. FrischMJ, TrucksGW, SchlegelHB, ScuseriaGE, RobbMA, CheesemanJR, ScalmaniG, BaroneV, MennucciB,. PeterssonGA, NakatsujiH, CaricatoM, LiX, HratchianHP, IzmaylovAF, BloinoJ, ZhengG, SonnenbergJL, HadaM, EharaM, ToyotaK, FukudaR, HasegawaJ, IshidaM, NakajimaT, HondaY, KitaoO, NakaiH, VrevenT, MontgomeryJA, PeraltaJE, OgliaroF, BearparkM, HeydJJ, BrothersE, KudinKN, StaroverovVN, KobayashiR, NormandJ, RaghavachariK, RendellA, BurantJC, IyengarSS, TomasiJ, CossiM, RegaN, MillamJM, KleneM, KnoxJE,. CrossJB, BakkenV, AdamoC, JaramilloJ,

GompertsR, StratmannRE, YazyevO, AustinAJ, CammiR, PomelliC, OchterskiJW, MartinRL, MorokumaK, ZakrzewskiVG, VothGA, SalvadorP, DannenbergJJ, DapprichS, DanielsAD, FarkasO, ForesmanJB, OrtizJ., CioslowskiJ, FoxDJ. Gaussian, Inc., Wallingford CT, 2009.

25. BeckeAD. Density-functional exchange-energy approximation with correct asymptotic behavior. Phys. Rev., 1988,A38: 3098-3100.
26. LeeC, YangW, ParrRG. Development of the Colle-Salvetti correlation-energy formula into a functional of the electron density. Phys. Rev., 1988,B37:785-789.
27. MiertusS, ScroccoE, TomasiJ.Electrostatic interaction of a solute with a continuum. *Chem. Phys., 1981, 55*: *117*–129.
28. TomasiJ, PersicoJ.Molecular Interactions in Solution: An Overview of Methods Based on Continous Distributions of the Solvent.Chem. Rev., 1994, 94: 2027-2094.
29. MarenichAV, CramerCJ, TruhlarDG.Universal solvation model based on solute electron density and a continuum model of the solvent defined by the bulk dielectric constant and atomic surface tensions.J. Phys. Chem., 2009, B113:6378-6396.
30. Ugliengo P. Moldraw Program, University of Torino, Dipartimento Chimica IFM, Torino, Italy, 1998.
31. Glendening E., Badenhoop JK, ReedAD, Carpenter JE, Weinhold F. NBO 3.1; Theoretical Chemistry Institute, University of Wisconsin; Madison, WI, 1996.
32. Bader RFW. Atoms in Molecules, A Quantum Theory, Oxford University Press, Oxford, 1990, ISBN: 0198558651.
33. Biegler-Köning F, Schönbohm J, Bayles D. AIM2000; A Program to Analyze and Visualize Atoms in Molecules. J. Comput. Chem., 2001,22:545.
34. BeslerBH, Merz Jr KM, Kollman PA. Atomic charges derived from demiempirical methods.J. Comp. Chem.,1990, 11: 431-439.
35. Parr RG, PearsonRG.Absolute hardness: companion parameter to absolute electronegativity.J. Am. Chem. Soc.,1983, 105: 7512-7516.
36. BrédasJ-L., Mind the gap! Materials Horizons,2014,1: 17–19.
37. Romani D, Brandán SA, Márquez MJ, Márquez MB.Structural, topological and vibrational properties of an isothiazole derivatives series with antiviral activities. J. Mol. Struct., 2015, 1100: 279-289.
38. Romani D, Tsuchiya S, Yotsu-Yamashita M,Brandán SA.Spectroscopic and structural investigation on intermediates species structurally associated to the tricyclic bisguanidine compound and to the toxic agent, saxitoxin.J. Mol. Struct., 2016, 1119: 25-38.
39. Romano E, Castillo MV, Pergomet JL, Zinczuk J, Brandán SA.Synthesis, structural and vibrational analysis of (5,7-Dichloro-quinolin-8-yloxy) acetic acid. J. Mol. Struct., 2012, 1018: 149–155.
40. Iramain MA, Davies L, Brandán SA.Structural and spectroscopic differences among the Potassium 5-hydroxypentanoyltrifluoroborate salt and the furoyl and isonicotinoyl salts. J Mol. Struct.,2019, 1176: 718-728.
41. IssaouiN, GhallaH, BrandánSA, BardakF, FlakusHT, AtacA, OujiaB. Experimental FTIR and FT-Raman and theoretical studies on the molecular structures of monomer and dimer of 3-thiopheneacrylic acid. J. Mol. Struct., 2017, 1135: 209-221.
42. Pulay P; Fogarasi G; Pongor *G*,Boggs JE; Vargha A. Combination of theoretical ab initio and experimental information to obtain reliable harmonic force constants. Scaled quantum mechanical (QM) force fields for glyoxal, acrolein, butadiene, formaldehyde, and ethylene.J. Am. Chem. Soc.,1983, 105:7073.
43. a) RauhutG, PulayP, Transferable Scaling Factors for Density Functional Derived Vibrational Force Fields.J. Phys. Chem., 1995, 99: 3093-3100. b) *Correction:* RauhutG, PulayP.J. Phys. Chem.,1995, 99: 14572.
44. SundiusT. Scaling of ab-initio force fields by MOLVIB. Vib. Spectrosc.,2002, 29 : 89-95.
45. KereszturyG, HollyS, BesenyeiG, VargaJ, WangAY, DurigJR.Vibrational spectra of monothiocarbamates-II. IR and Raman spectra, vibrational assignment, conformational analysis and *ab initio* calculations of *S*-methyl-*N,N*-dimethylthiocarbamate. Spectrochim. Acta, 1993, 49A : 2007-2026.
46. MichalskaD, Wysokinski. The prediction of Raman spectra of platinum(II) anticancer drugs by density functional theory. Chemical Physics Letters, 2005, 403 : 211-217.
47. Infrared and ATR spectra of 2C-B available from: file:///D:/2C-B/Articles/4-bromo-2,5-dimethoxyphenethylamine.pdf.
48. Bohloko NS. Development and formulation of an intranasal dosage form for cyclizine hydrochloride. Doctoral Thesis, Faculty of Health Sciences at the Department of Pharmaceutics, Potchefstroom University for Christian Higher Education, Potchefstroom, 2003.
49. Xiang Li. (E)-N-(3,4-Dimethoxyphenethyl)-3-methoxybut-2-enamide. ActaCryst.,2010,. E66, o432.
50. Leyton P, Paipa C, Berrios A, Zárate A, Castillo MV, Brandán SA.Vibrational study and DFT calculations of 2-[[5-amino-5-oxo-2-(phenylmethoxycarbonylamino) pentanoyl] amino] acetic acid.J. Mol. Struct.,2013, 1031: 110-118.
51. ContrerasCD, LedesmaAE, LanúsHE, ZinczuckJ, BrandánSA.Hydration of L-tyrosine in aqueous medium. An experimental and theoretical study by mixed quantum mechanical/molecular mechanics methods.Vibrat. Spectr.,2011, 57: 108-115.
52. LeytonP, BrunetJ, SilvaV, PaipaC, CastilloMV, BrandánSA..An experimental and theoretical study of L-Tryptophan in aqueous solution combining two-layered ONIOM and SCRF calculations.Spectrochim. Acta Part A,2012, 88: 162-170.
53. RoldánML, LedesmaAE, RaschiAB, CastilloMV, RomanoE, BrandánSA. A new experimental and theoretical investigation on the structures of aminoethylphosphonic acid in aqueous medium based on the vibrational spectra and DFT calculations. J. Molec. Struct., 2013, 1041: 73-81.
54. Guzzetti K, Brizuela AB, Romano E, Brandán SA.Structural and vibrational study on zwitterions of L-threonine in aqueous phase using the FT-Raman and SCRF calculations. J. Molec. Struct. , 2013, 1045: 171-179.
55. GatfaouiS, IssaouiN, BrandánSA, RoisnelT, MarouaniH. Synthesis and characterization of p-

xylylenediaminiumbis(nitrate). Effects of the coordination modes of nitrate groups on their structural and vibrational properties. J Mol. Struct.,2018, 1151: 152-168.

56. Minteguiaga M, Dellacassa E, Iramain MA, Catalán CAN, BrandánSA.A structural and spectroscopic study on carquejol, a relevant constituent of the medicinal plant Baccharistrimera (Less.) DC. (Asteraceae). J. Mol. Struct., 2017, 1150 : 8-20.
57. Minteguiaga M, Dellacassa E, Iramain MA, Catalán CAN, Brandán SA.FT-IR, FT-Raman, UV-Vis, NMR and structural studies of Carquejyl Acetate, a component of the essential oil from *Baccharistrimera* (Less.) DC. (Asteraceae).J Mol. Struct.,2019, 1177: 499-510.
58. Minteguiaga M, Dellacassa E, Iramain MA, Catalán CAN, Brandán SA.Synthesis, spectroscopic characterization and structural study of 2-isopropenyl-3-methylphenol, carquejiphenol, a carquejol derivative with potential medicinal use.J Mol. Struct.,2018,1165: 332-343.

How to cite this article:

María Eugenia Manzur *et al* (2019) 'Evaluatingproperties of Free Base, Cationic and Hydrochloride Species of Potent Psychotropic 4-Bromo-2,5-Dimethoxyphenethylamine Drug', *International Journal of Current Advanced Research,* 08(03), pp.17921-17934. DOI: http://dx.doi.org/10.24327/ijcar.2019.17934.3416

****